Multiphysics Modeling of a Metal Foam

B. Chinè[*1,2], M. Monno[1,3]
[1] Laboratorio MUSP, Macchine Utensili e Sistemi di Produzione, Piacenza, Italy, [2]Instituto Tecnològico de Costa Rica, Cartago, Costa Rica, [3]Politecnico di Milano, Dipartimento di Meccanica, Milano, Italy.
*Corresponding author: Laboratorio MUSP, Via Tirotti 9, 29122, Piacenza, Italy, bruno.chine@musp.it

Abstract: In metal foam processing nucleated gas bubbles expand in a heated metal, then the foam cools and solidifies. In this work we use Comsol Multiphysics 4.2 to study heat transfer, growth and movement of hydrogen gas bubbles in liquid aluminium for a metal foam expanding in a 2D mold. In the model, the bubble growth is simulated by using a specific expansion rate, then the movement of hydrogen gas bubbles in liquid aluminium is numerically computed by using the equations of fluid dynamics coupled to the level set method. In spite of the problem complexity and the needed simplifications, the computational model is very well suited to describe satisfactorily heat transfer, bubble expansion, interface movement and fluid flow during the foaming process. Interesting considerations can be drawn regarding the temperature field in the system, the influence of the mold geometry and the resulting expansion of the metal foam.

Keywords: bubble expansion, metal foam, multiphase flow, level set.

1. Introduction

Metal foams are interesting materials with many potential applications. Foamed metals or alloys include gas voids in the material structure and as a result introduce density ρ as a new variable, with the real possibility to modify ad hoc their physical properties. Therefore, a wide range of possibilities arise in the automotive, aerospace, nautical, railway, building, civil engineering and medical industries. For industrial applications, metal foams offer attractive combinations of low density, high stiffness to weight ratio, good energy absorption and vibration damping capacity.

Many different processes have been developed for producing metal foams [1]. To produce this cellular material, a liquid metal (e.g. Al) could be *foamed directly* by injecting gas (H_2) or gas releasing blowing agents (solid particles), or by producing supersaturated metal-gas solutions. Also, it is possible to manufacture foamed component via the powder metallurgical route, i.e. starting from a compacted mixture (precursor) of metal (or metal alloy) and blowing agent powders, such as Al and titanium hydride (TiH_2) (*indirect foaming via precursor)*. Remelting the precursor leads to in situ gas evolution within the metal as the blowing agents release H_2 gas. With this process, closed molds can be filled with foam, and structural foam parts of complex shape can be manufactured. Shaped sandwich panels with two dense face sheets and a cellular core can also be made [1].

Our research interest is in the indirect foaming process carried out in a furnace, where a simultaneous mass, momentum and energy transfer between three phases, solid, liquid and gas, has to be taken into account. These mechanisms can be modelled and studied by applying computational techniques, although the computational work is very challenging. On the other hand these phenomena have major effects on the quality of metal foams. In fact, during mold filling, the desired metal foam density is dependent on the ability of controlling the precursor heating, pore formation and inflation, liquid drainage, bubbles coalescence and on the final foam solidification to prevent the foam collapse.

Our multiphysics modelling work starts analyzing the heat transfer to the precursor, then computes the H_2 bubbles growth and their movement in melted Al for a metal foam expanding in a 2D mold. To accurately compute the evolution of the gas-liquid interfaces during foam expansion, we use the Eulerian numerical formulation provided by the level set method, which embeds the interface as the zero level set of a function, a method having encountered extensive applications in multiphase flow modelling.

To model and numerically solve the governing equations of the problem, we use Comsol Multiphysics 4.2, in particular the heat transfer module [2] and the level set interface

together with the weakly-compressible flow, both available in the CFD module [3].

2. Model specification

Even with the aid of numerical tools, the simulation of an indirect foaming process via precursor is very complex, due to the presence of several and simultaneous physical phenomena. Under heat treatment, at temperatures near the melting point of the matrix material, the blowing agent decomposes and the released gas forces the compacted precursor material to expand. In the process, the resulting foam expansion depends on the content of blowing agent, temperature T, time t, pressure p, heating rate, size of the precursor, etc. Other conditions govern the dynamics of the gas bubbles in the matrix, such as the matrix state (solid, semi-solid or liquid), viscosity η of the fluid, drainage of liquid material towards downer areas, coalescence between bubbles, presence of solid particles on the bubble walls, etc. The next sections 2.1 and 2.2 give a description of the model and the assumptions done to reasonably simplify the problem.

2.1 Physical model

We consider a 2D solid section (disk of radius R_P) of a precursor (compacted mixture of Al with a low content of TiH_2 -approximately 0.5 wt. %), partially filling a circular shaped mold of AISI 4340 steel, as depicted in Figure 1. The mold is placed horizontally inside a furnace, therefore we exclude gravity and drainage effects in the model. Across the solid walls, which have two different thickness (the larger one for the upper wall), two small symmetrical openings are provided in the mold, thus maintaining a constant pressure in the cavity.

At the beginning the mold is at ambient temperature T_0 in the furnace, and no gas bubbles are present in the solid matrix of the precursor (beginning of *step 1*). The empty regions in the mold are considered to be completely filled with H_2 gas, keeping the air out of the computations and allowing us to restrict the multiphase flow to only two fluids, H_2 and liquid Al. Next, after assuming that the temperature of the external side of the mold equals suddenly the furnace operating temperature T_{EXT}, heat will be transferred inside the mold cavity and

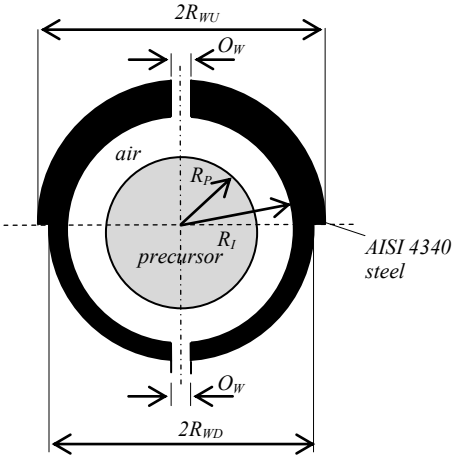

Figure 1. Precursor (Al + TiH_2) of a metal foam placed in a mold. In the computations the air of the cavity is substituted by H_2.

phenomena such as gas releasing, pore formation and inflation will be stimulated.

Some simplifications are made in the model regarding bubbles nucleation and growth. In fact, the mechanism behind pore formation during the foaming process is still not understood, but it accepted that plays a key role in the quality of the evolving structure. Local pore formation occurs at the locations of individual blowing agents, on the other hand non local formation represents the pore formation in other locations in the precursor material. Combinations of these mechanisms are also possible, as shown by Rack et al. [4] using synchrotron based microtomography and 3D image analysis. The authors pointed also out that two temperature ranges are fundamental for pore nucleation during foaming: the first one corresponds to the temperature interval in which H_2 is released, whilst the second one is related to the melting temperature of Al or the melting temperature range for an Al alloy. We simplify each range to a unique value, respectively called T_R and T_M. Depending on the relative values of T_R and T_M, H_2 could be delivered in a fully melted Al if $T_R > T_M$ (for an alloy T_M is the *liquidus* temperature) or in a solid Al matrix if $T_R < T_M$ (for an alloy T_M is the *solidus* temperature). Obviously, the gas H_2 would instead flow in a semi-molten material if the blowing agent releases gas when the temperature of the system lies in the *solidus-liquidus* interval of the Al alloy.

Therefore, after applying the operating furnace temperature on the mold walls, the model consider heat transfer (conductive, convective and radiative) in order to compute the precursor temperature in time. Thus, when the value of T_R is reached, the model assumes that H_2 bubbles are formed instantaneously inside the solid matrix (beginning of *step 2*), while heat continues to flow from the mold walls to the precursor. We suppose also that bubble are not able to expand when the matrix is still solid.

Later, when the precursor temperature is equal to T_M (the melting temperature of Al), the correspondent region is now liquid and the bubbles start to grow and flow (beginning of *step 3*). Tension surface effects govern now the interface equilibrium. With the precursor now melted, the expansion of the H_2 gas, considered immiscible in the Al liquid, is introduced in the model using a specific expansion rate and taking the movement of the interfaces into account. Actually, in this step of the foaming process a global density variation $\rho_G = \rho_G(t)$ for the H_2 gas could be prescribed or obtained by means of experimental measurements in similar conditions.

Finally, phase change phenomena and relative energies are neglected in the model.

2.2 Mathematical model

We select a 2D Cartesian system of rectangular coordinates (*x, y*) and apply an axial symmetry condition around the *y* axis. With this assumption, the foaming process takes place in a 2D region (semicircle Ω_I of radius R_I), separated from the exterior by two mold walls, upper and downer, of external radius R_{WU} and R_{WD} respectively (Figure 2). The semicircle Ω_I and the two mold walls form the computational region Ω of this study. As described early, three different steps have been supposed for the metal foaming process: *step 1* ($T_0 \le T < T_R$), *step 2* ($T_R \le T < T_M$) and *step 3* ($T_M \le T < T_{EXT}$).

In the model, as long as the precursor is not melted (*steps 1* and *2*), the coupled partial differential equations for the fluid dynamics and heat transfer problems are the following:

$$\frac{\partial \rho}{\partial t} + \nabla \cdot (\rho \mathbf{u}) = 0 \qquad (1)$$

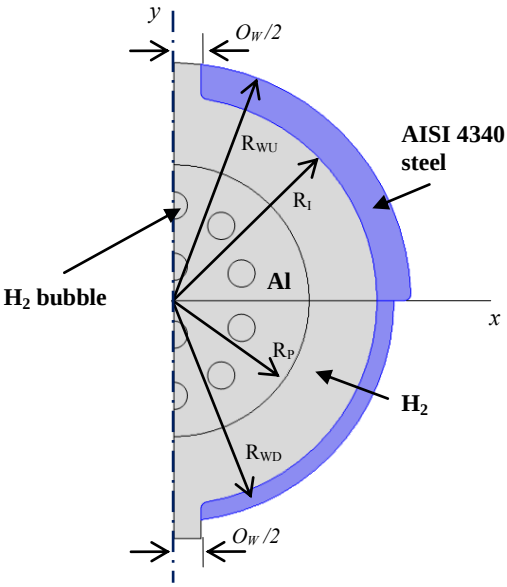

Figure 2. Model of precursor (Al + H_2) and mold, with the initial position of N (=12) H_2 bubbles for the simulation of *steps 2* and *3*. The cavity is considered also filled with H_2.

$$\rho \frac{\partial \mathbf{u}}{\partial t} = \nabla \cdot [-p\mathbf{I} + \eta(\nabla \mathbf{u} + (\nabla \mathbf{u})^T) - \frac{2\eta}{3}(\nabla \cdot \mathbf{u})\mathbf{I}] + \mathbf{F} \qquad (2)$$

$$\rho C_p \frac{\partial T}{\partial t} + \rho C_p \mathbf{u} \nabla T = \nabla \cdot (k \nabla T) + Q \qquad (3)$$

where $\mathbf{u}$ is the velocity field, $\mathbf{F}$ the body forces (null in our case), while k, C_p and Q, are the thermal conductivity, the specific heat capacity at constant pressure and the heat source other than viscous heating, respectively. Compressibility of the gas in the cavity is computed with a weakly-compressible model, valid for gas flows with low Mach numbers (approximately $Ma < 0.3$). The flow is then assumed laminar, because the velocities are very low (~ 10^{-5} m/s, only thermal expansion), as well as the resulting Reynolds number Re. For the same reason, a Stokes flow regime is supposed. The conductive heat transfer across the solid walls of the mold is simulated by putting $\mathbf{u} = \mathbf{0}$ in the above equations. Initial and boundary conditions complete then the mathematical model. As initial conditions, temperature $T = T_0$ and velocity $\mathbf{u} = \mathbf{0}$ are prescribed elsewhere. On the other hand, the conditions used for the

boundary of Ω are $T = T_{EXT}$ and $\mathbf{u} = \mathbf{0}$ on the external and internal mold wall, respectively. On the small openings, we set Dirichlet conditions $T = T_{EXT}$ and $p = 0$ with vanishing viscous stresses. Radiative heat transfer is computed between precursor and internal mold wall, by assuming a transparent, no participating media between them with their surfaces as opaque to radiation. When the precursor temperature is equal to T_R, a number N of small circular regions of Ω are then considered as N gas bubbles (Figure 2).

In *step 3*, once the expansion starts, both the growth of the N gas bubbles embedded in the viscous liquid and the successive expansion of the precursor are modelled using the classical equations of fluid dynamics coupled to the level set method. In addition, the simultaneous heat transfer mechanism is still considered. Therefore, the coupled partial differential equations of the model are the previous equations (1) and (3), while the momentum transport equation (2) is modified by putting $\mathbf{F} = \mathbf{F}_{ST}$, with $\mathbf{F}_{ST}$ being the surface tension force acting at the interface between the two fluids. The liquid Al is considered to be an incompressible Newtonian fluid, while the density variation of the compressible H_2 gas is defined by giving an explicit expression to the equation:

$$\rho_G = \rho_G(t) \qquad (4)$$

Laminar flow and Stokes hypothesis could be considered still valid. In metal foams processing, the effective viscosity of the melted fluid surrounding the gas bubble depends, other than on the temperature, on the presence of solid particles next to the bubble walls. More exactly, the viscosity of the surrounding fluid is almost one –two orders of magnitude higher than the aluminium viscosity. Gergely and Cline [5] used a liquid viscosity of 0.4 Pa·s for a melted aluminum with solid particles, when simulating a metal foam obtained via the melted route. For a gas bubble of initial diameter $D_{G,0}$ = 10^{-3} m, expanding in liquid Al of density ρ_L = 2.4x10^3 kg/m^3, we have:

$$\mathrm{Re} = \frac{U_L D}{\upsilon_L} = 0.24 \qquad (5)$$

considering a velocity U_L = 10^{-2} m/s with a dynamic viscosity η_L of 10^{-1} Pa·s, giving a kinematic viscosity $\upsilon_L = \frac{\eta_L}{\rho_L} = \frac{1}{2.4} x10^{-4}$ m^2/s.

The model is completed by the following equation for the level set function ϕ:

$$\frac{\partial \phi}{\partial t} + \mathbf{u} \cdot \nabla \phi = \gamma \nabla \cdot [\varepsilon \nabla \phi - \phi(1-\phi)\frac{\nabla \phi}{|\nabla \phi|}] \qquad (6)$$

which describes the advection of ϕ. In Comsol a signed distance function at $t = 0$ is used to build the function ϕ which corresponds to the interface at the level set $\phi = 0.5$. With the same method, the values of ϕ inside the two phases are setting as $0 \le \phi < 0.5$ for one fluid (in our model is Al) and $0.5 < \phi \le 1$ for the other one (H_2 gas). In Eq. 6 γ represents the reinitialization parameter and controls the re-initialization performed at some later point in the calculation beyond $t = 0$ (need to preserve the values of distance close to the interface), while ε is the interface thickness parameter which adds extra numerical diffusion in order to stabilize the computations of Eq. 6. Finally, initial and boundary conditions are provided for the partial differential equations used in *step 3*. Regarding the initial conditions, we assume that velocity and temperature fields are those computed at the end of the second step. Moreover, in the gas regions we set an initial pressure $p_{G,0} = \sigma / R_{G,0}$ and a null velocity. Finally, the same boundary conditions of *step 1* and *2* are considered, except for the velocity on the inner mold wall, where a slip condition is now exploited.

3. Solution with Comsol Multiphysics

The model equations are numerically solved with Comsol Multiphysics 4.2, using the heat transfer module [2] and the level set interfaces together with the weakly-compressible flow of the CFD module [3]. The computational domain is obtained by meshing the region Ω with nearly 3x10^5 triangle elements. Three computational models are carried out for the three different steps of the metal foaming process described previously in section 2.1 and whose

mathematical formulation has been given in section 2.2.

The first model uses the Conjugate Heat Transfer interface, solving the coupled heat transfer and fluid dynamics problem during *step 1*, evaluating the precursor temperature in different areas by means of domain probes. The second model exploits the same interface, but introduces N static gaseous regions in the computations, monitoring the precursor temperature via domain probes to run properly the *step 2* of the process. For *step 3*, a third model uses the CFD module with the level set method which is very well suited to describe the interface movement during the gas expansion. Moreover, two others interfaces, Heat Transfer in Solids and Heat Transfer in Fluids, are added to solve the partial differential equations of the simultaneous heat transfer problem. In the first heat transfer interface, a convective cooling boundary conditions is set on the inner solid wall of the mold, to model the heat flux leaving the solid domain and coming in the fluid. A reciprocal inward boundary condition is provided for the same heat flux in the second heat transfer interface. Radiative heat transfer is now neglected, although it is possible to incorporate it in the convective heat flux to the precursor.

4. Experimental results and discussion

Table 1 gives geometrical dimensions and physical properties of the materials used in the simulations and depicted in Figures 1 and 2. Other parameters of the model are shown in Table 2. We assume that the expansion rate has a exponential pattern $\rho_G(t) = \exp(-t)$, although experimentally evaluated rates can be tested. The maximum mesh size was set to $1.3\text{x}10^{-4}$ m, corresponding to around $3.4\text{x}10^{5}$ degrees of freedom for the calculations of *steps 1* and *2* and $1.83\text{x}10^{6}$ degrees of freedom for those of *step 3*. In both cases, the direct solver PARDISO has been used. The convergence obtained during some computations was good: starting with a time step of 10^{-6} s and 10^{-2} s for *step 1* and *step 2* respectively, the final step-size was of 31 s for the first and of 58 s for the second step. On the contrary, the time step was close to 10^{-2} s for *step 3*, but in this case this value is strictly dependent on the parameters of Table 1, which directly affect the foam flow. In particular, the time step is automatically reduced by the solver when merging phenomena between bubbles occur in the flow. In this case the time step was

Table 1: Geometrical dimensions and properties of the materials used in the numerical computations ((*) = from Comsol Material Data Base).

Magnitude	Symbol	Value
External radius of the upper mold wall	R_{WU}	35 mm
External radius of the downer mold wall	R_{WD}	32.5 mm
Internal radius of the mold	R_I	30 mm
Opening width	O_W	8 mm
Precursor radius	R_P	20 mm
AISI 4340 density (*)	ρ_M	7850 kg/m^3
AISI 4340 thermal conductivity (*)	k_M	44.5 W/ (m·K)
AISI 4340 specific heat capacity at p=const (*)	$C_{P,M}$	475 J/(kg ·K)
Ambient pressure	p_{EXT}	0 Pa
Ambient temperature	T_0	300 K
Furnace temperature	T_{EXT}	973.15 K
Gas releasing temperature	T_R	650 K
Al melting temperature	T_M	933.15 K
Steps 1 and 2		
H_2 density (*)	ρ_G	ρ_G *(p.T-ideal gas)*
H_2 viscosity (*)	η_G	η_G *(T)*
H_2 thermal conductivity (*)	k_G	k_G *(T)*
H_2 specific heat capacity at p=const (*)	$C_{P,G}$	$C_{P,G}$ *(T)*
Al (solid) density (*)	ρ_S	2700 kg/m^3
Al (solid) thermal conductivity (*)	k_S	160 W/(m ·K)
Al (solid) specific heat capacity at p=const (*)	$C_{P,S}$	900 J/(kg ·K)
Al (solid, oxidized) surface emissivity	E_S	0.2
AISI 4340 (oxidized) surface emissivity	E_M	0.8
Step 3		
Number of H_2 bubbles	N	12
Initial bubble radius	$R_{G,0}$	2 mm
Initial H_2 density	$\rho_{G,0}$	1 kg/m^3
H_2 density variation	$\rho_G(t)$	exp*(-t)*
H_2 viscosity	η_G	10^{-2} Pa·s
Al (liquid) density	ρ_L	1 kg/m^3
Al viscosity	η_L	10^{-1} Pa·s
Surface tension coefficient	σ	0.9 N/m

Table 2. Other model parameters used in the numerical computations.

Magnitude	Symbol	Value
Max element size of the mesh	-	$1.3\text{x}10^{-4}$ m
Time stepping	-	set by the solver
Relative tolerance	-	10^{-3}
Absolute tolerance	-	10^{-4}
Interface thickness	ε	$1\text{x}10^{-4}$ m
Reinitialization	γ	0.1 m/s

set to approximately 10^{-5} s. The computational model was run in a PC with Intel Xenon CPU E5620, 8 core, 2.40 GHz, 48 GB RAM, 64bit and Windows 7 Operative System. The solution time is of $2.6\text{x}10^{3}$ s for *step 1* and of 750 s for *step 2*, while for *step 3* is around 10^{5} s, for N=12 bubbles and a simulated expansion of 1.942 s.

In metal foaming simulation, the strong property gradients at fluid interfaces cause calculations to be carried out with some difficulties, as experimented by the same authors during previous numerical tests ([6], [7]). Very refined meshes and high computational performances are needed for capturing these gradients and accurately simulating the bubbles interactions, especially when several bubbles are present in the system. In *step 3*, we use an initial density ratio $\rho_L/\rho_{G,0}$ of 1, with a corresponding initial kinematic viscosities ratio $\upsilon_L/\upsilon_{G,0}$ of 10. However, limiting the foaming process to the expansion of one bubble, a ratio $\frac{\rho_L}{\rho_G}=\frac{2400}{0.02647}$ with a corresponding ratio $\frac{\upsilon_L}{\upsilon_{G,0}}=\frac{10^{-1}}{10^{-2}}\bullet\frac{0.02647}{2400}$ has been simulated satisfactorily.

Figures 3 and 4 show the temperature field in the system at the end of *step 1* (t = 300 s) and *step 2* (t = 875 s), respectively. The temperature field is uniform, because the different wall thickness of the mold only control the energy transfer in the first instants of the heating process, afterwards radiation mechanisms begin to counterbalance.

During *step 3*, the expansion of H_2 bubbles in the precursor gives peculiar phenomena. For example, a mergence between the first two

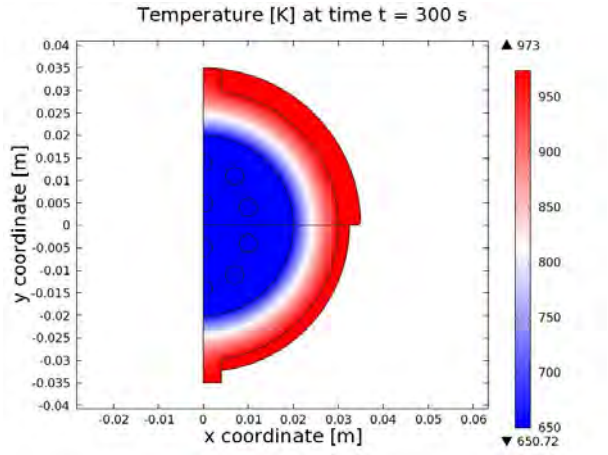

Figure 3. Temperature field at the end of *step 1*, when the gas releasing temperature of 650 K is reached in the precursor.

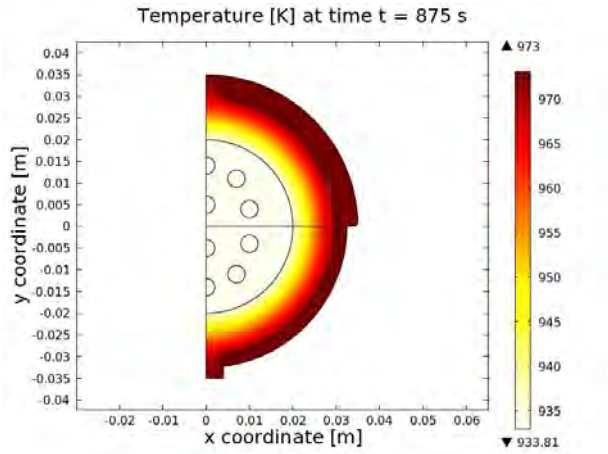

Figure 4. Temperature field at the end of *step 2*, when the Al melting temperature of 933.15 K is reached in the precursor.

bubbles occurs 1.593 s after the growth is started, accelerating the fluid (Figure 5). Because the disjoining pressure has been not considered, no repulsive effects can act against the bubbles coalescence [8]. As we said before, the solver automatically reduces the time step in order to catch these very fast processes. Figure 6 plots the volume fraction of H_2 at time t =1.942 s. We observe that four H_2 bubbles have merged and the expansion is more pronounced in x direction, thus the foam evidencing a typical flattening of its circular surface.

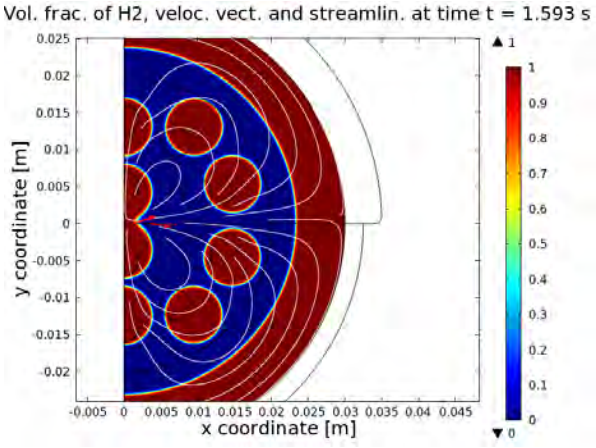

Figure 5. Acceleration of liquid Al during the mergence between two H_2 bubbles, after 1.593 s the expansion is started.

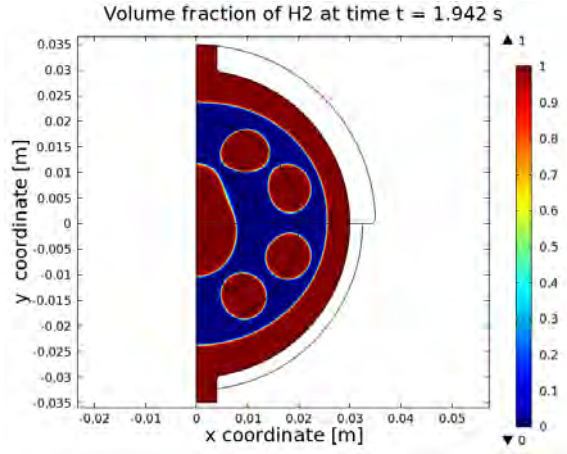

Figure 6. Volume fraction of H_2 after 1.942 s the expansion is started, with mergence of four H_2 bubbles occurred in the central region of the precursor.

5. Conclusions

A model by Comsol Multiphysics has been presented for the simulation of a metal foam manufactured by an indirect foaming process via precursor. Heat transfer, growth and movement of H_2 gas bubbles in liquid Al has been modelled for a metal foam expanding in a 2D mold. When the precursor melts, growth of H_2 gas is introduced in the model using a specific expansion rate, the movement of the interfaces is taken into account and surface tension effects are considered. The numerical findings verify that the computational model, based on a level set technique, can be effective for modeling the foaming process of a metal. However, other physical mechanisms as heating and cooling rates, drainage, disjoining pressure and final solidification of the foam should be included for a more comprehensive model. We think to extend the work, taking these mechanisms into account and including mass diffusion as a tool to foresee the correct expansion rate. Finally, when developing more comprehensive models for a foaming process, computational requirements have to be considered.

6. References

[1] J. Banhart, Manufacture, characterization and application of cellular metals and metal foams, *Progress in Materials Science*, **46**, 559-632 (2001).

[2] Comsol AB, Comsol Multiphysics-Heat Transer Module, *User's Guide*, **Version 4.2,** (2011).

[3] Comsol AB, Comsol Multiphysics-CFD Module, *User's Guide*, **Version 4.2,** 201-264 (2011).

[4] A. Rack, H.M. Helwig, A. Bütow, A. Rueda, B. Matijašević-Lux, L. Helfen. J. Goebbels and J. Banhart, Early pore formation in aluminium foams studied by synchrotron-based microtomography and 3-D image analysis, *Acta Materalia*, **57**, 4809-4821 (2009).

[5] V. Gergely and T.W. Clyne, Drainage in standing liquid metal foams: modeling and experimental observations, *Acta Materialia*, **52**, 3047-3058 (2004).

[6] B. Chinè and M. Monno, A model of gas bubble growth by Comsol Multiphysics, *Proceedings of 2010 European Comsol Conference*, Paris, (2010).

[7] B. Chinè and M. Monno, Multiphysics modeling of a gas bubble expansion, *Proceedings of 2011 European Comsol Conference*, Stuttgart, (2011).

[8] C. Körner, *Integral Foam Molding of Light Metals,* 124. Springer-Verlag, Berlin Heidelberg (2008).

7. Acknowledgements

Authors gratefully acknowledge the collaboration provided by Dr. Valerio Marra and the staff of Comsol AB, Brescia, Italy.